Combining a BCL2 Inhibitor with the Retinoid Derivative Fenretinide Targets Melanoma Cells Including Melanoma Initiating Cells

Nabanita Mukherjee[1], Steven N. Reuland[1], Yan Lu[1], Yuchun Luo[1], Karoline Lambert[1], Mayumi Fujita[1], William A. Robinson[2], Steven E. Robinson[2], David A. Norris[1,3,4] and Yiqun G. Shellman[1,4]

Investigations from multiple laboratories support the existence of melanoma initiating cells (MICs) that potentially contribute to melanoma's drug resistance. ABT-737, a small molecule BCL-2/BCL-XL/BCL-W inhibitor, is promising in cancer treatments, but not very effective against melanoma, with the antiapoptotic protein MCL-1 as the main contributor to resistance. The synthetic retinoid fenretinide *N*-(4-hydroxyphenyl)retinamide (4-HPR) has shown promise for treating breast cancers. Here, we tested whether the combination of ABT-737 with 4-HPR is effective in killing both the bulk of melanoma cells and MICs. The combination synergistically decreased cell viability and caused cell death in multiple melanoma cells lines (carrying either BRAF or NRAS mutations) but not in normal melanocytes. The combination increased the NOXA expression and caspase-dependent MCL-1 degradation. Knocking down NOXA protected cells from combination-induced apoptosis, implicating the role of NOXA in the drug synergy. The combination treatment also disrupted primary spheres (a functional assay for MICs) and decreased the percentage of aldehyde dehydrogenase ^{high} cells (a marker of MICs) in melanoma cell lines. Moreover, the combination inhibited the self-renewal capacity of MICs, measured by secondary sphere-forming assays. *In vivo*, the combination inhibited tumor growth. Thus, this combination is a promising treatment strategy for melanoma, regardless of mutation status of BRAF or NRAS.

Journal of Investigative Dermatology (2015) **135,** 842–850; doi:10.1038/jid.2014.464; published online 4 December 2014

INTRODUCTION

Metastatic melanoma is a devastating disease resistant to conventional therapies. Despite several recent Food and Drug Administration-approved drugs for melanomas, there is still a pressing need for therapies using novel approaches (Chapman *et al.*, 2011; Garbe *et al.*, 2011; Arbiser *et al.*, 2012; Finn *et al.*, 2012; Wong *et al.*, 2013). It is proposed that cancer stem cells, or cancer initiating cells (CICs), are responsible for initiation, progression, and resistance to treatment (Lee *et al.*, 2014). Recent studies provide evidence that a subpopulation of melanoma cells possess characteristics similar to CICs, termed melanoma initiating cells (MICs) (Fang *et al.*, 2005; Monzani *et al.*, 2007; Roesch *et al.*, 2010; Civenni *et al.*, 2011; Santini *et al.*, 2012). We previously demonstrated the existence of human melanoma cells that fulfill the criteria for MICs (self-renewal and differentiation), and these cells are more resistant to chemotherapy (Luo *et al.*, 2012). As a strategy in preventing relapse, it is crucial to look for therapies that de-bulk melanoma tumors and also target MIC populations.

The BCL2 (BCL-2) family is important in regulating the intrinsic apoptotic pathway and includes three groups: (1) antiapoptotic proteins BCL-2, BCL2L (BCL-XL), BCLW (BCL-W), MCL1 (MCL-1), A1, and BCL-B; (2) multi-domain pro-apoptotic proteins BAX, BAK, and BOK, which are effectors of apoptosis; and (3) BH3-only pro-apoptotic proteins BIM, PUMA, BAD, NOXA, BIK, BMF, and tBID, which are initiators of apoptosis (see review (Czabotar *et al.*, 2014)). Interactions between different members are not mutually exclusive or equal. Some BH3-only proteins only bind to one group of anti-apoptotic proteins—e.g., NOXA only binds to MCL-1/A1 and BAD only to BCL-2/BCL-XL/BCL-W. Conversely, BIM, PUMA, and tBID bind to multiple antiapoptotic proteins. These various combinations of interactions control the initiation of apoptosis.

The antiapoptotic BCL-2 protein family contributes to melanoma's resistance to apoptosis (Soengas and Lowe, 2003; Eberle and Hossini, 2008; Placzek *et al.*, 2010; Haass and Schumacher, 2014; Mohana-Kumaran *et al.*, 2014), and

[1]*Department of Dermatology, University of Colorado Anschutz Medical Campus, School of Medicine, Aurora, Colorado, USA;* [2]*Division of Medical Oncology, University of Colorado Anschutz Medical Campus, School of Medicine, Aurora, Colorado, USA and* [3]*Department of Veterans Affairs Medical Center, Dermatology Section, Denver, Colorado, USA*

[4]*These authors contributed equally to this work.*

Correspondence: Yiqun G. Shellman, Department of Dermatology, University of Colorado Anschutz Medical Campus, School of Medicine, Mail Stop 8127, Aurora, Colorado 80045, USA.
E-mail: Yiqun.Shellman@ucdenver.edu

Abbreviations: ALDH, aldehyde dehydrogenase; CIC, cancer initiating cell; MIC, melanoma initiating cell; PARP, poly (ADP-ribose) polymerase; PDX, patient-derived xenograft; 4-HPR, N-(4-hydroxyphenyl)retinamide

Received 16 May 2014; revised 3 October 2014; accepted 6 October 2014; accepted article preview online 28 October 2014; published online 4 December 2014

clinical trials targeting antiapoptotic Bcl-2 family members are currently underway (Thomas *et al.*, 2013). ABT-737 and its oral bioactive form, ABT-263, are small molecule BCL-2/BCL-XL/BCL-W inhibitors that show promising results in cancer therapy, either alone or in combination with other chemotherapeutics (Oltersdorf *et al.*, 2005; Thomas *et al.*, 2013). However, many labs, including ours, found that ABT-737 by itself is not very effective for de-bulking melanoma and that the antiapoptotic protein MCL-1 is the primary contributor to resistance (Miller *et al.*, 2009; Reuland *et al.*, 2011, 2012). Therefore, compounds targeting MCL-1 are good potential partners to be combined with ABT-737.

To combine with ABT-737, we chose fenretinide *N*-(4-hydroxyphenyl)retinamide (4-HPR) for its ability to inhibit MCL-1 indirectly and for its killing action in CICs of other cancers (Torrisi and Decensi, 2000; Kang *et al.*, 2008; Zhang *et al.*, 2013). This combination has synergistic cytotoxicity in other cancers (Kang *et al.*, 2008; Fang *et al.*, 2011; Bruno *et al.*, 2012); however, it has never been tested on melanoma cell lines or any CIC populations.

One of the common ways of isolating or enriching CICs is by the use of surface markers (Shakhova and Sommer, 2013; Stecca *et al.*, 2013). However, the use of surface markers like CD271 or CD133 to enrich MICs has produced contradictory results (Shakhova and Sommer, 2013). To avoid such issues, we used three surface-marker–independent assays to examine the effects of drug treatments on the MIC populations: primary sphere-forming, secondary-sphere forming, and the Aldefluor assays. Melanoma spheres display ''stemness,'' exhibit self-renewal capacity and tumorigenicity, and sustain tumor growth *in vivo*, allowing for the generation of human melanoma xenografts (Santini *et al.*, 2012; Stecca *et al.*, 2013). We used a primary sphere-forming functional assay to test drug potency on melanoma cells harboring stem-like features, the MICs. Post drug treatment, and using the cells from the primary sphere assay, a secondary sphere assay described by Stecca *et al.*, 2013 quantified the self-renewal capacity of the enriched, resistant MICs. Furthermore, we and others established that cells with higher aldehyde dehydrogenase (ALDH) activity are enriched in MICs (Luo *et al.*, 2012; Santini *et al.*, 2012). Therefore, we used the Aldefluor assay to further examine the effects of drug treatments on MICs.

The present study tested the effects of a combination melanoma treatment with ABT-737 (a small molecule BCL-2/BCL-XL/BCL-W inhibitor) and 4-HPR (an indirect MCL-1 inhibitor), focusing on de-bulking the melanoma and killing MICs and/or inhibiting their self-renewal capacity.

RESULTS

4-HPR and ABT-737 synergistically reduced cell viability and increased apoptosis in melanoma cells but not in melanocytes

To explore whether treatment with 4-HPR and ABT-737 affected the cell viability and apoptosis of the melanoma cells, we used the MTS assay, the Annexin V assay, and bright-field morphological analysis (Figure 1). The data from the MTS assays were analyzed with Calcusyn to obtain the combination index (CI) value for all of the combinations (Supplementary Table S1 online). The combination treatment was strongly synergistic over a wide range of drug concentrations, with CI values <0.3 for all melanoma cell lines tested. Cells treated with various doses of 4-HPR and ABT-737 showed synergy occurring from 5 to 10 μM 4-HPR and at or above 1.1 μM ABT-737 for all cell lines, except A375, which showed synergy at much lower 4-HPR doses (Figure 1a and Supplementary Table 1 online). The Annexin V assay demonstrated that a combination of 4-HPR and 3.3 μM ABT-737 caused marked apoptosis in every melanoma cell line we tested, ranging from ~40 to 70%, even though the single agents had little effect (Figure 1b). The combination induced similar effects in the melanoma cell lines carrying mutated BRAF or NRAS and significantly increased the percentage of Annexin V^+ cells for all melanoma cell lines tested ($P<0.01$). Melanoma cells treated with the combination showed signs of cell death, such as detachment from the substrate, misshape morphology, and blebbing, whereas melanocytes remained largely unaffected (Figure 1c). Moreover, the primary melanocyte line HEM_NLP2 was resistant to the drug combination (Figure 1a and b). The immortalized melanocyte line PIG1 showed only modest effects at the highest doses (Figure 1a). Overall, the above assays indicated that the combination treatment synergistically reduced cell viability and caused cell death in multiple melanoma cell lines but not in melanocytes.

The combination induced caspase-dependent MCL-1 degradation and increased NOXA expression

We and others have shown that MCL-1 is the primary protein that allows melanoma's resistance to ABT-737, but an increase in NOXA expression or a decrease in MCL-1 expression overcomes this resistance (Miller *et al.*, 2009; Reuland *et al.*, 2011; Lucas *et al.*, 2012; Reuland *et al.*, 2012). Only the combination treatment notably increased NOXA expression and cleaved poly (ADP-ribose) polymerase (PARP) (Figure 2a). In addition, only the combination treatment decreased the levels of MCL-1 (Figure 2a). Quantification indicated that the combination treatment markedly increased the NOXA/MCL-1 ratio by at least 5-fold in all the melanoma cell lines tested (Figure 2a).

Various triggers induce caspase-mediated MCL-1 degradation, contributing to accelerated apoptosis (Miller *et al.*, 2009; Ramirez-Labrada *et al.*, 2014). We examined this potential mechanism using a pan-caspase inhibitor as described (Miller *et al.*, 2009; Ramirez-Labrada *et al.*, 2014). Co-treatment of the pan-caspase inhibitor Z-VAD-FMK with the combination blocked caspase 3 activity and PARP cleavage, as expected. MCL-1 expression also increased in the combination-treated cells to a level close to the control cells, suggesting that the MCL-1 degradation is mediated by caspases (Figure 2b). Thus, these data suggest that the combination induced expression of pro-apoptotic NOXA and caspase-dependent degradation of antiapoptotic protein MCL-1. Results were similar in both BRAF mutated (451Lu) and NRAS mutated cells (WM852c and SK-MEL-30).

Inhibition of NOXA lessened the effects of the drug combination

We examined the killing potency of the combination of 4-HPR and ABT-737 on cells after knocking down NOXA, BIM, BID,

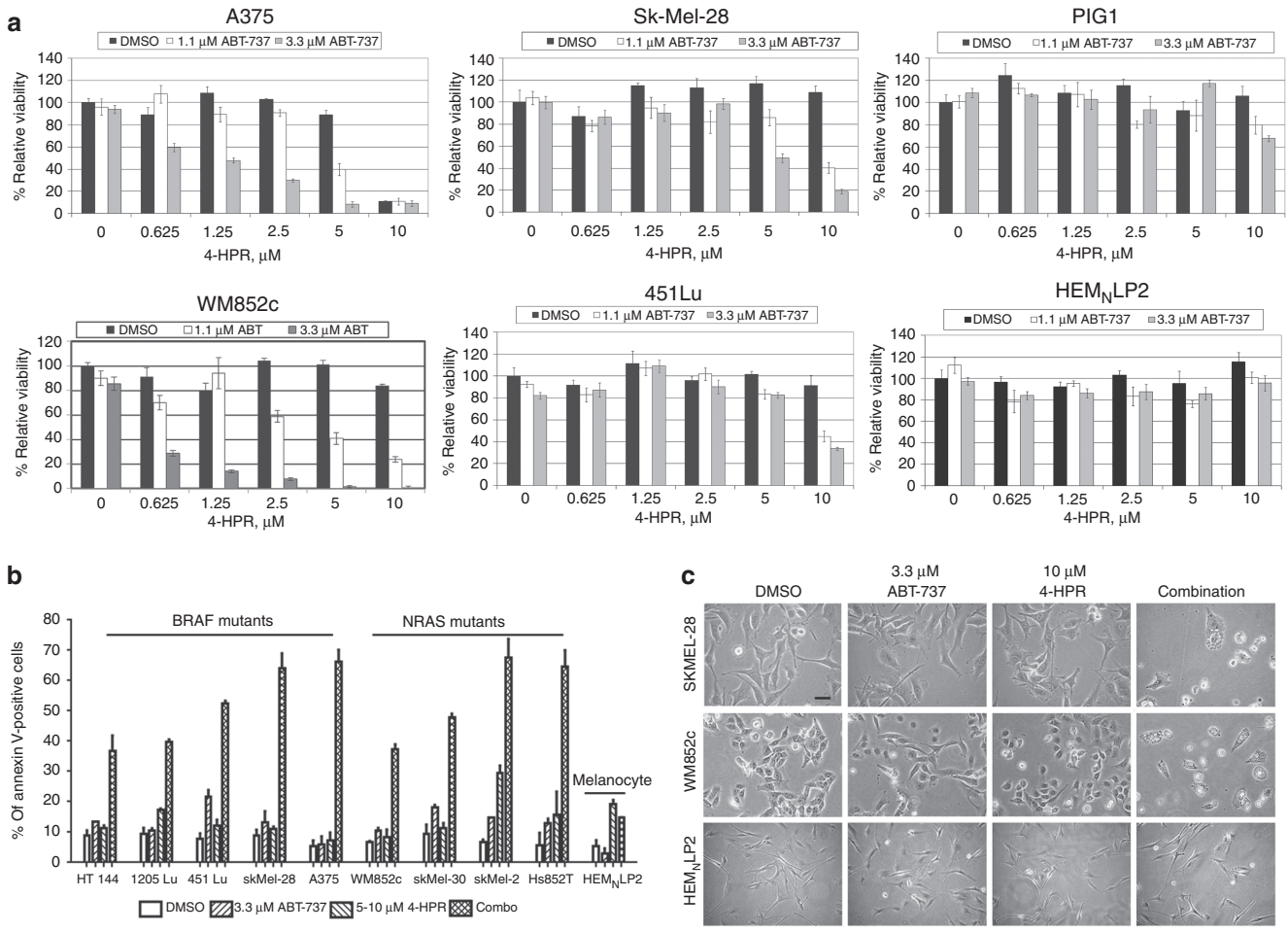

Figure 1. The effects of 4-HPR combined with ABT-737 in melanomas and melanocytes. (**a**) The MTS assay shows that 4-HPR combined with ABT-737 synergistically killed melanomas (A375, SK-MEL-28, WM852c, and 451Lu) but had little effect on melanocytes (HEM_NLP2 and PIG1). Cells were treated with the indicated drugs for 48 hours before the MTS assay. (**b**) The annexin V assay shows massive apoptosis in melanoma cells induced by 48-hour treatment of 4-HPR and ABT-737. In all melanoma cells (either mutant BRAF or NRAS), the combination treatment significantly induced apoptosis compared with all other treatments (DMSO or single drug, $P<0.01$). (**c**) Visual appearance of cells showing cell death in combination treatments for melanoma cells but not for melanocytes. Scale bar = 100 μm.

PUMA, or TP53 (p53) (Figure 3). Of these, only knockdown of NOXA resulted in a significant reduction in cell death compared with the control in all the cell lines tested ($P<0.05$), although the protections were not complete (Figure 3a–d, and supplementary Figure S1 online). In addition, knockdown of BIM significantly protected SK-MEL-30 ($P<0.01$) but not A375 cells, even though the knockdown efficiency seemed to be compatible. Interestingly, BIM expression was higher in SK-MEL-30 than in A375 cells (Supplementary Figure S2 online). These data suggest that the combination-induced killing is NOXA dependent, and BIM may have a role in a cell-line–dependent manner.

The combination of 4-HPR with ABT-737 caused cytotoxicity in MICs and also increased the NOXA/MCL-1 ratio in sphere cultures of multiple melanoma cell lines

We examined whether this combination is also effective against MICs using sphere-forming and the Aldeflour assays (Figure 4). In all of the nine melanoma cell lines, the combination severely disrupted the primary spheres compared with the control ($P<0.001$, Figure 4a and b). The combination also significantly decreased the number of spheres as compared with ABT-737 alone in eight of the cell lines ($P<0.001$) and as compared with 4-HPR in two of them ($P<0.05$ or lesser, Figure 4b). 4-HPR significantly decreased the sphere numbers in all the cell lines ($P<0.01$ or lesser) and ABT-737 significantly decreased the number in 1205Lu, WM852c, and Hs852T compared with DMSO ($P<0.01$).

In eight out of nine melanoma cell lines, the combination significantly decreased the percentage of $ALDH^{high}$ cells compared with the DMSO control ($P<0.01$ or less) (Figure 4c). In seven out of nine melanoma cell lines, the combination significantly decreased the percentage of $ALDH^{high}$ cells compared with ABT-737 ($P<0.05$) (Figure 4c). In Hs852T and SK-MEL-2, the combination significantly decreased the percentage of $ALDH^{high}$ cells compared with DMSO,

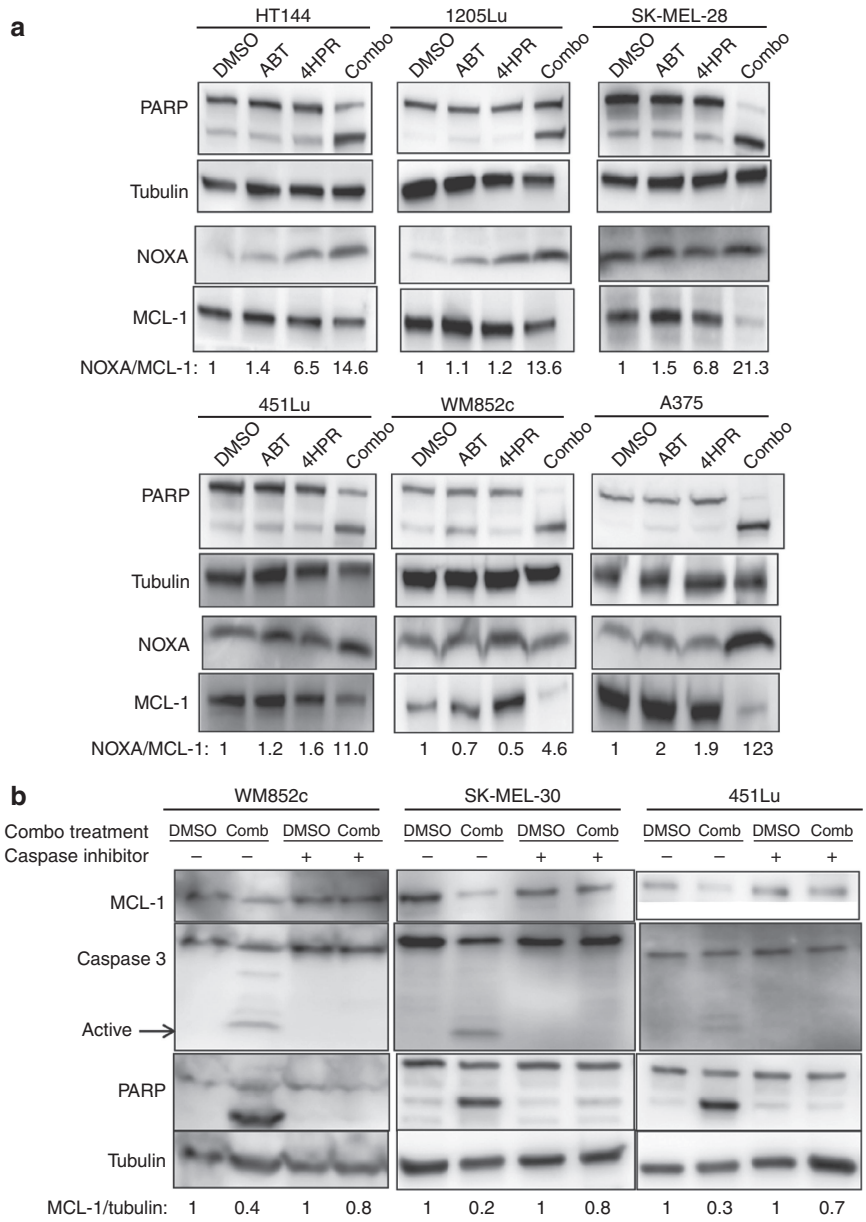

Figure 2. The combination of 4-HPR with ABT-737 induced PARP cleavage, increased the NOXA/MCL-1 ratio, and caused Caspase-mediated MCL-1 degradation. (**a**) Immunoblot of cell lysates treated with either vehicle control (DMSO), 3.3 μM ABT-737 (ABT), 5–10 μM 4-HPR (4HPR), or the combination of the two drugs (Combo). The ratio of NOXA/MCL-1 in the control was set as ''1'' for each cell line. (**b**) Immunoblot of cell lysates treated with either vehicle control (DMSO) or the combination with or without co-treatment of 30 μM pan caspase inhibitor Z-VAD-FMK. WM852c and SK-MEL-30 are NRAS mutants, and all other cell lines shown here are BRAF mutants. The normalized MCL-1 levels in the Combo with or without the Caspase inhibitor were compared with the respective DMSO conditions.

ABT-737, as well as 4-HPR ($P<0.05$ or lesser) (Figure 4c). Consistent with these results, the combination also reduced JARID1B expression (Supplementary Figure S3 online), another potential marker for MICs (Roesch *et al.*, 2013). Interestingly, single treatment of ABT-737 increased the JARID1B expression compared with control in one of the cell lines.

With the sphere lysates, we then performed immunoblot (Figure 4d). The data were similar to our findings in monolayer conditions; the combination treatment increased the expression of NOXA and cleaved PARP and decreased the expression of MCL-1 (Figure 4d vs. Figure 2). Similarly, knockdown of NOXA also reduced the effects of the combination treatment in the sphere-forming ability of multiple cell lines (Figure 4e and Supplementary Figure S4 online). Taken together, results indicate that the combination treatment induced NOXA-dependent cytotoxicity in the MIC population.

4-HPR combined with ABT-737 inhibited the self-renewal capacity of MICs in multiple melanoma cell lines *in vitro*

One cause of cancer relapse is the self-renewal capacity of CICs (Beck and Blanpain, 2013); the secondary sphere formation assay is a means of measuring this capacity *in vitro*.

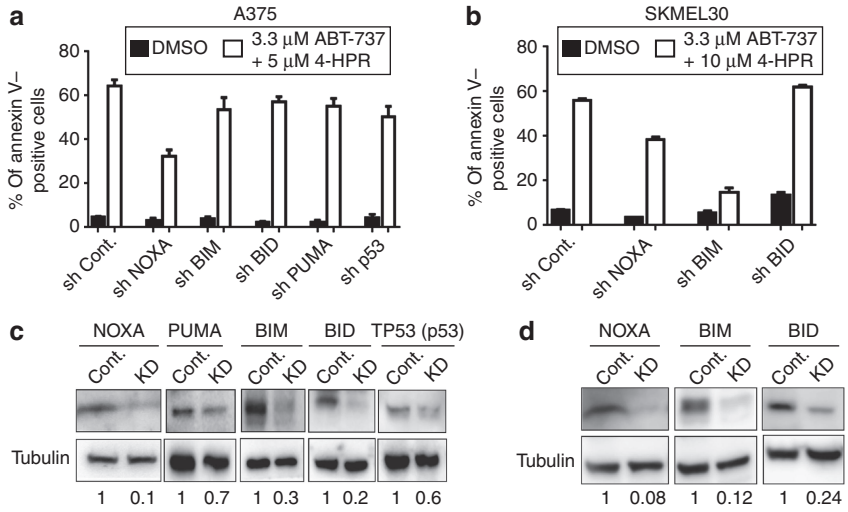

Figure 3. Knockdown of NOXA decreased drug-induced cell death. Annexin V assays of the indicated knockdown cell lines derived from A375 (**a**) or SK-MEL-30 (**b**). Immuoblots (**c**, **d**) of lysates from the cell lines used in **a** and **b,** respectively show efficient knockdown of indicated proteins. In A375, knockdown of NOXA by shRNA (shNoxa) significantly reduced combination-induced apoptosis as compared with control (shCont) ($P<0.05$), but knockdown of other pro-apoptotic proteins did not. In SK-MEL-30, both knockdown of NOXA and BIM significantly reduced combination-induced apoptosis as compared with control ($P<0.01$).

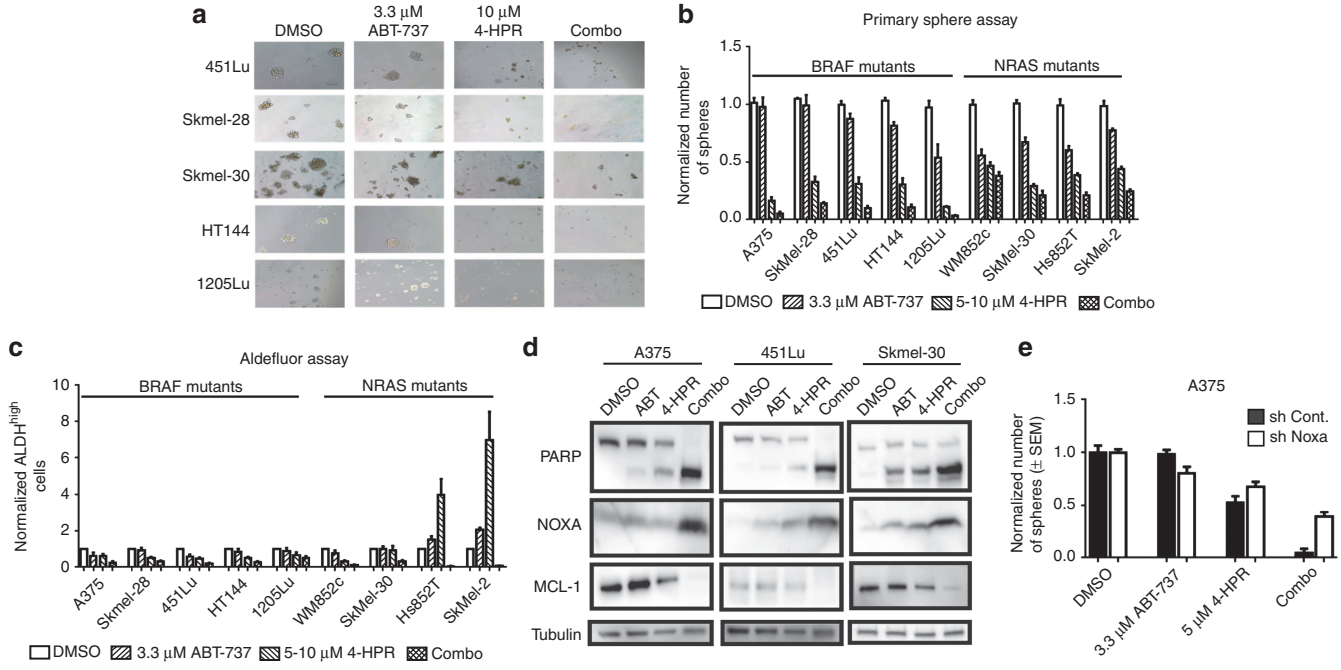

Figure 4. The combination of 4-HPR with ABT-737 caused cytotoxicity in melanoma initiating cells. (**a**) Bright-field analysis showing complete disruption of primary spheres after 48 hours of the combination treatment. Scale bar = 100 μm. (**b**) Quantification of the number of spheres from melanoma cell lines with either mutant BRAF or NRAS. The combination significantly reduced the number of spheres compared with the vehicle (DMSO) or ABT-737 in multiple melanoma cell lines ($P<0.001$). (**c**) Quantification of the ALDH assay. The combination treatment significantly reduced the relative percentage of ALDH^{high} cells compared with the control or ABT-737 in multiple melanoma cell lines. (**d**) Immunoblots of lysates from the cells used in **b** showing that the combination induced PARP cleavage, increased NOXA, and reduced MCL-1. (**e**) Primary sphere assays with NOXA knockdown (shNoxa) or control (shCont.) of A375 after being treated with indicated drugs. Knockdown of NOXA significantly protected cells from the combination-induced disruption of spheres compared with the control ($P<0.01$).

Instead of just enriching stem-like cells, as in the primary sphere-forming assay, this assay measures the cell population's ability to regenerate after drug treatment. Primary spheres formed after indicated drug treatments were dissociated and replated at the same viable cell density. However, no drugs were added during the secondary sphere-forming assay. This

assay specifically assesses if any of the remaining cells—those that escaped chemotherapeutics—are capable of self-renewing and regenerating into a mass of tumor cells.

The most striking and consistent result across all cell lines was that the combination treatment almost eliminated all secondary sphere formation. Interestingly, unlike in the primary sphere assay, 4-HPR treatment alone did not significantly inhibit the formation of the secondary spheres in most of the cell lines (Figure 5a), indicating that 4-HPR did not kill a subpopulation of MICs capable of proliferation post drug treatment. Statistical analyses indicated that the combination treatment significantly decreased the number of secondary spheres formed compared with DMSO ($P<0.01$), ABT-737 ($P<0.01$), or 4-HPR treatment ($P<0.05$ or less) in all seven cell lines (Figure 5b). Furthermore, single drug treatments showed an increased number of secondary spheres, compared with the control in some of the BRAF mutated cell lines (Figure 5c), although the *P*-value reached significance only in the 451Lu ($P<0.05$).

Visualization of these cells with EtBr/AO staining indicated that the majority of cells in the control or single drug treatments were alive, but the majority of cells in the combination treatments were dead (Figure 5b). Thus, the results show that the combination prevented the formation of secondary spheres in multiple cell lines, demonstrating that the combination decreased MIC's self-renewal capability.

In patient-derived samples, 4-HPR combined with ABT-737 significantly disrupted spheres

To determine whether the combination treatment of ABT-737 with 4-HPR had a similar effect on samples more clinically relevant than cell lines, we examined the effects of the combination in patient tumor samples maintained in a tumor xenograft mouse model (patient-derived xenograft (PDX)). Drug–responses more closely match clinical outcomes in the PDX model, and the PDX model provides more material compared with fresh tumor tissues (Tentler *et al.*, 2012). Drug treatment was tested in four patient samples that we established in a PDX model for melanoma (Luo *et al.*, 2012). Spheres took longer to form in most of patient-derived cells, delaying the start of drug treatment, but otherwise cells were handled in the same way. Interestingly, the effects of the combination treatment on primary sphere formation were more similar to the effects of secondary sphere formation of the melanoma cell lines. In the PDX model cells, primary spheres were severely disrupted (Figure 6a), with significantly reduced sphere numbers compared with all other treatment conditions: DMSO ($P<0.001$), ABT-737 ($P<0.01$ or less), and 4-HPR ($P<0.01$ or less) (Figure 6b).

4-HPR and ABT-737 reduce tumor growth in an *in vivo* mouse xenograft model

In a mouse xenograft model, the rate of tumor growth in the combination group was significantly slower compared with

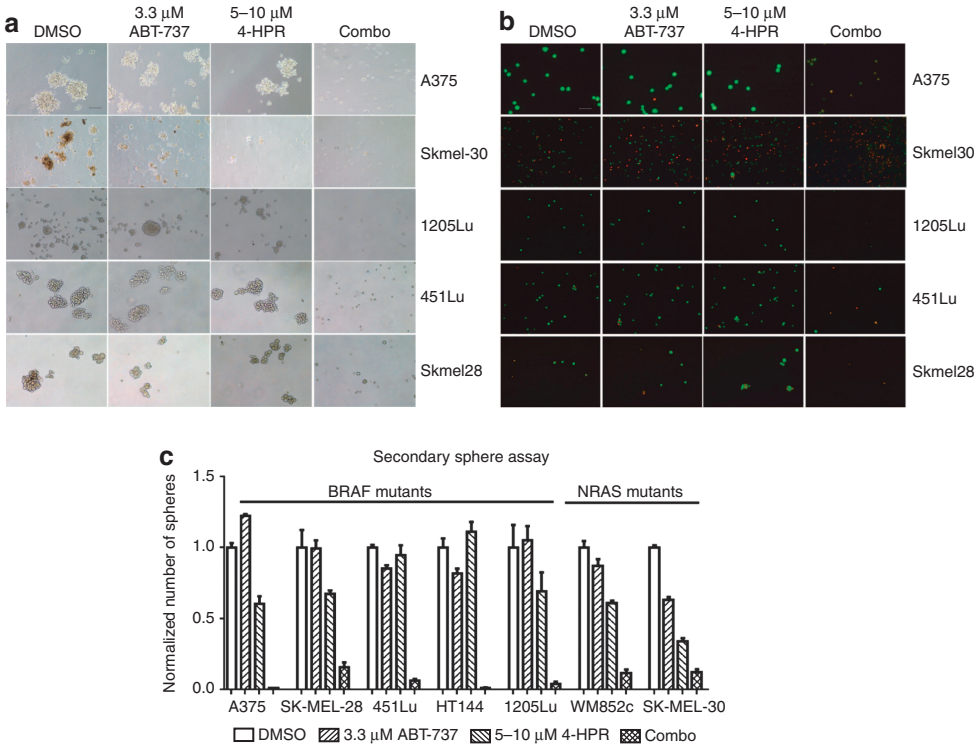

Figure 5. The Combination of 4-HPR and ABT-737 inhibited the self-renewal capacity of MICs *in vitro*. (**a**) Bright-field analysis of the secondary sphere assay showing that only the combination inhibited the formation of secondary spheres. Scale bar = 100 μm. (**b**) Visualization of the cells with ethidium bromide/acridine orange (EtBr/AO) staining indicated that the majority of cells in the control or single drug treatment were alive (green), but the majority of cells in the combination were dead (orange). Scale bar = 100 μm. (**c**) Quantification of the number of secondary spheres from melanoma cell lines with either mutated BRAF or NRAS. The combination significantly reduced the number of spheres compared with all other treatments in multiple melanoma cell lines ($P<0.05$ or less).

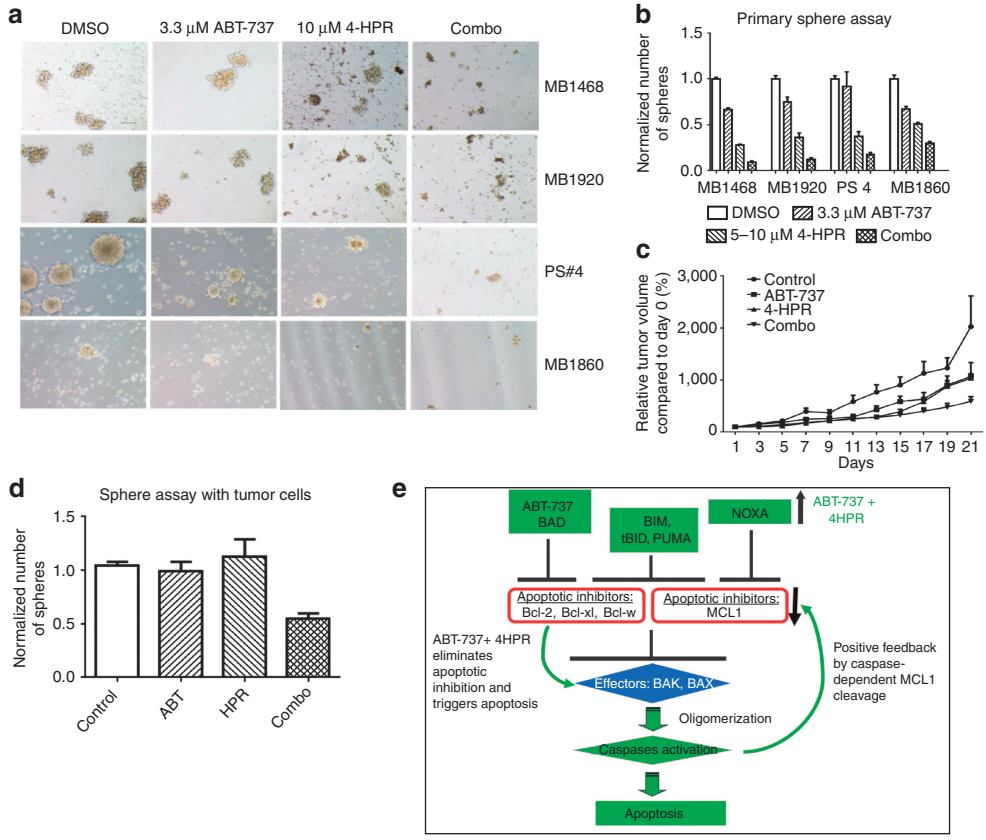

Figure 6. The combination of 4-HPR with ABT-737 had cytotoxic effects in patient-derived xenograft (PDX) tumor samples and in a mouse xenograft model. (**a**) Bright-field analysis of PDX tumor samples showing complete disruption of spheres after 48 hours of combination treatment. Scale bar = 100 μm. (**b**) Quantification of the number of spheres for the PDX samples. The combination treatment significantly reduced the number of spheres compared with vehicle (DMSO, $P<0.001$)), ABT-737 ($P<0.01$ or less), and 4-HPR ($P<0.01$ or less) in multiple PDX samples. (**c**) Relative tumor volumes in a mouse xenograft model. The tumor volume at day 0 was set as 100%. The combination significantly inhibited the tumor growth compared with control and 4-HPR. (**d**) Sphere assays with the tumor cells collected at the end of the xenograft experiment from **c**. The combination significantly reduced the number of spheres compared with vehicle or individual treatments ($P<0.05$). The graph represents the mean of three different sets of tumors collected. (**e**) A simplified model to illustrate how the combination of ABT-737 plus 4HPR triggers apoptosis by altering Bcl-2 family members. Initially, the combination eliminates the functions of multiple apoptotic inhibitors and activates apoptosis in two ways: ABT-737 alone blocks BCL-2/BCL-XL/BCL-W, and the combination induces NOXA expression, which inhibits MCL-1. Consequently, the combination treatment's synergistic mechanism is achieved by MCL-1 degradation by a small percentage of activated caspases, which produces a positive feedback signal for further apoptosis activation.

the control group ($P=0.002$), with no significant difference in the tumor growth rate among the control, ABT-737 alone, or 4-HPR alone groups. At the end of the treatment period on days 19 and 21, the relative tumor volume of the combination group was significantly reduced compared with both the control group ($P<0.001$) and the 4-HPR alone group ($P<0.05$) (Figure 6d). Single-drug treatments, ABT-737 or 4-HPR alone, were not significantly different from the control. These results show that the combination of ABT-737 and 4-HPR significantly reduced the growth of melanoma tumors *in vivo* compared with vehicle or individual drugs (Figure 6c).

To determine whether treatments *in vivo* also affect tumor cells' capacity to form spheres, we performed sphere-forming assays with the single cell suspensions isolated from the surviving tumors of the above experiment. No drugs were added to the cells during the sphere assay. These mouse-xenograft–derived tumor cells took longer compared with the cell lines to form spheres, and the combination significantly reduced the number of spheres compared with vehicle or individual treatments ($P<0.05$) (Figure 6d). Immunoblots show that the combination induced PARP cleavage and increased the NOXA/MCL-1 ratio (Supplementary Figure 5 online), similar to the *in vitro* results.

DISCUSSION

This study examined the effects of combining ABT-737 with 4-HPR on melanoma, looking at the efficacy of killing both the bulk of tumor cells and the MICs. Regarding de-bulking the tumor cells, we confirmed by MTS assays, Annexin V assays, and the detection of PARP cleavage by immunoblot that the combination treatment synergistically decreased cell viability and induced apoptosis in multiple cells lines (Figures 1 and 2). Moreover, BRAF or NRAS status did not affect the sensitivity to the drug combination. Given the lack of treatment options for

NRAS mutated melanomas, it is exciting that this combination may lead to better patient outcomes.

To examine the effect on MIC populations, we utilized primary and secondary sphere formation assays and an ALDH activity assay. In multiple melanoma cell lines, the combination and 4-HPR alone significantly disrupted the primary spheres and decreased the percentage of $ALDH^{high}$ cells, compared with vehicle (DMSO) and ABT-737. Strikingly, only the combination significantly inhibited the formation of secondary spheres in these cells. The primary spheres and $ALDH^{high}$ cell populations are enriched in MICs, but the secondary sphere assay measures the capacity of self-renewal. Only the combination treatment significantly decreased self-renewal capacity, preventing proliferation post treatment, essentially inhibiting the regrowth of tumor cells. Thus, the combination was more potent compared with the control or either drug alone in eliminating MICs and has the potential to prevent relapse in melanoma patients.

Overall, in melanoma cell lines and PDX patient samples, the combination treatment, but not individual treatments, is cytotoxic to the bulk of melanoma cells and more importantly to the MICs. This treatment would potentially hinder relapse by blocking tumor regeneration. Collectively, results of *in vitro* monolayer, sphere and ALDH assays, and mouse *in vivo* all show that the combination treatment vigorously kills melanoma cells and MICs compared with vehicle or the single drug.

We investigated several potential mechanisms for the synergistic effects between ABT-737 and 4-HPR in melanomas. Although 4-HPR is known to cause cell death by inducing reactive oxygen species and ceramide synthesis (Maurer *et al.*, 2000), our results indicated that reactive oxygen species or ceramide were not involved in melanoma death (Supplementary Figures 6 and 7 online). Instead, the combination induced caspase-dependent MCL-1 degradation and increased NOXA expression (Figure 2). Changes in the expression of NOXA and MCL-1 were similarly observed in both mutated BRAF and NRAS melanomas and may serve as biomarkers of sensitivity to the combination treatment. Moreover, blocking NOXA expression partially protected multiple melanoma cell lines from the combination (Figure 3 and Supplementary Figure 1 online). Thus, our data suggest that this drug combination induces cell death in melanoma by antagonizing multiple antiapoptotic BCL-2 family members, including BCL-2, BCLXL, and BCL-W (by ABT-737) and MCL-1 (by induction of NOXA and caspase-dependent MCL-1 degradation) (Figure 6e). Consequently, a small amount of activated caspases led to further degradation of MCL-1, producing a positive feedback signal for further activation of apoptosis, as seen in the combination-induced synergy (Figure 6e).

Currently, two leading activation models, direct and indirect, address how interactions between members of the BCL-2 family regulate the activation of apoptosis (Czabotar *et al.*, 2014). The consensus is that these two models are not mutually exclusive, and the predominant pathway depends on the biological context (Czabotar *et al.*, 2014). In the direct activation model, certain BH3-only proteins directly activate the effectors BAX and BAK, and antiapoptotic BCL-2 members primarily sequester BH3-only proteins. In the indirect model, BAX and BAK become activated only if all of the antiapoptotic proteins are neutralized by BH3-only proteins. Our results are consistent with the indirect activation model.

We have tested a few combinations with ABT-737 previously and found that combination with proteasome inhibitor Velcade was very toxic (Miller *et al.*, 2009; Reuland *et al.*, 2011, 2012), and the MIC populations were quite resistant to TMZ (Luo *et al.*, 2012). In contrast, 4-HPR is considered a chemoprevention agent because of its low toxicity (Malone *et al.*, 2003). Moreover, current targeted melanoma treatments, with PLX4032 for instance, only kill tumor cells harboring BRAF mutations. Of BRAF carriers, the response rate is 50% and relapse is all too common. Consequently, melanoma oncology is in dire need of multiple therapies using novel mechanistic approaches that target non-BRAF mutated tumors or heterogeneous populations within the same melanoma. The combination of 4-HPR and ABT-737 may provide a potent treatment option, regardless of mutation status.

MATERIALS AND METHODS

Primary and secondary sphere-forming assays

All sphere assays were performed with poly-hema (Sigma, St Louis, MO) coated plates or dishes (Reginato *et al.*, 2003), in stem cell media as described previously (Dontu *et al.*, 2003; Iwanaga *et al.*, 2012). Specifically, the media contained DME/F12 (Hyclone, South Logan, UT) supplemented with B27 (Invitrogen, Grand Island, NY), 20 ng ml^{-1} EGF and 20 ng ml^{-1} bFGF (BD Biosciences, Redford, MA), and 4 μg ml^{-1} heparin (Sigma).

Primary sphere assay. Cells were plated at a density of 1–5 viable cell μl^{-1} for melanoma cell lines and 20 viable cell μl^{-1} for the patient samples. Fresh medium was added every 2–3 days. The criteria described in the study by Stecca *et al.*, (2013) were used to define a sphere. Briefly, a sphere is a compact spherical-roundish mass of cells with an approximate diameter greater than 50 μm. The spheres were treated with indicated drugs on day 5. After 48 hours, the numbers of spheres were counted.

Secondary sphere assay. Primary spheres, formed as mentioned above for indicated drug treatments, were dissociated into single cells and replated as described in the study by Stecca *et al.*, (2013). The procedures were the same as for the primary sphere assay, except that no drugs were added during the secondary sphere assays. At least three repeats of both the primary and secondary sphere assays were carried out for each cell line. The data were normalized as the relative fold compared with the vehicle (DMSO) control, and the number of spheres in the DMSO control was set at ''1''. The ethidium bromide/acridine orange staining assay, as described previously (Ribble *et al.*, 2005; Smith *et al.*, 2012), was used to estimate live, dead, or apoptotic cells of the secondary spheres dissociated with phospate-buffered saline-EDTA (Stecca *et al.*, 2013).

Other methods

Further information about other materials and methods is provided in the Supplementary Material online.

CONFLICT OF INTEREST

The authors declare no conflict of interest.

ACKNOWLEDGMENTS

This work was supported in part by a Veterans Administration merit grant from the Department of Veterans Affairs (Veterans Health Administration, Office of Research and Development, Biomedical Laboratory Research and Development) to DAN, by a Southwestern Skin Cancer SPORE Pilot project to YGS, and by NIH training grant 5T32AR007411-29 to SNR (PI: DAN). We thank the University of Colorado Skin Cancer Biorepository for providing human melanoma samples and melanoma cell lines. We are grateful to Karen Helm, Christine Childs, and Lester Acosta of the CU Cancer Center Flow Cytometry Core facility (supported by Cancer Center Support Grant P30CA046934 and NIAMS Skin Disease Research Core Center grant P30 AR 057212) for their expert technical assistance. We thank Abbott Laboratories (Saul Rosenberg, Steven Elmore, and colleagues) for providing the ABT-737 compound.

SUPPLEMENTARY MATERIAL

Supplementary material is linked to the online version of the paper at http://www.nature.com/jid

REFERENCES

Arbiser JL, Bips M, Seidler A *et al.* (2012) Combination therapy of imiquimod and gentian violet for cutaneous melanoma metastases. *J Am Acad Dermatol* 67:e81–3

Beck B, Blanpain C (2013) Unravelling cancer stem cell potential. *Nat Rev Cancer* 13:727–38

Bruno S, Ghiotto F, Tenca C *et al.* (2012) N-(4-hydroxyphenyl)retinamide promotes apoptosis of resting and proliferating B-cell chronic lymphocytic leukemia cells and potentiates fludarabine and ABT-737 cytotoxicity. *Leukemia* 26:2260–8

Chapman PB, Hauschild A, Robert C *et al.* (2011) Improved survival with vemurafenib in melanoma with BRAF V600E mutation. *N Eng J Med* 364:2507–16

Civenni G, Walter A, Kobert N *et al.* (2011) Human CD271-positive melanoma stem cells associated with metastasis establish tumor heterogeneity and long-term growth. *Cancer Res* 71:3098–109

Czabotar PE, Lessene G, Strasser A *et al.* (2014) Control of apoptosis by the BCL-2 protein family: implications for physiology and therapy. *Nat Rev Mol Cell Biol* 15:49–63

Dontu G, Abdallah WM, Foley JM *et al.* (2003) In vitro propagation and transcriptional profiling of human mammary stem/progenitor cells. *Genes Dev* 17:1253–70

Eberle J, Hossini AM (2008) Expression and function of bcl-2 proteins in melanoma. *Curr Genomics* 9:409–19

Fang D, Nguyen TK, Leishear K *et al.* (2005) A tumorigenic subpopulation with stem cell properties in melanomas. *Cancer Res* 65:9328–37

Fang H, Harned TM, Kalous O *et al.* (2011) Synergistic activity of fenretinide and the Bcl-2 family protein inhibitor ABT-737 against human neuroblastoma. *Clin Cancer Res* 17:7093–104

Finn L, Markovic SN, Joseph RW (2012) Therapy for metastatic melanoma: the past, present, and future. *BMC Med* 10:23

Garbe C, Eigentler TK, Keilholz U *et al.* (2011) Systematic review of medical treatment in melanoma: current status and future prospects. *Oncologist* 16:5–24

Haass NK, Schumacher U (2014) Melanoma never says die. *Exp Dermatol* 23:471–2

Iwanaga R, Wang CA, Micalizzi DS *et al.* (2012) Expression of Six1 in luminal breast cancers predicts poor prognosis and promotes increases in tumor initiating cells by activation of extracellular signal-regulated kinase and transforming growth factor-beta signaling pathways. *Breast Cancer Res* 14:R100

Kang MH, Wan Z, Kang YH *et al.* (2008) Mechanism of synergy of N-(4-hydroxyphenyl)retinamide and ABT-737 in acute lymphoblastic leukemia cell lines: Mcl-1 inactivation. *J Natl Cancer Inst* 100:580–95

Lee N, Barthel SR, Schatton T (2014) Melanoma stem cells and metastasis: mimicking hematopoietic cell trafficking? *Lab Invest* 94:13–30

Lucas KM, Mohana-Kumaran N, Lau D *et al.* (2012) Modulation of NOXA and MCL-1 as a strategy for sensitizing melanoma cells to the BH3-mimetic ABT-737. *Clin Cancer Res* 18:783–95

Luo Y, Dallaglio K, Chen Y *et al.* (2012) ALDH1A isozymes are markers of human melanoma stem cells and potential therapeutic targets. *Stem Cells* 30:2100–13

Malone W, Perloff M, Crowell J *et al.* (2003) Fenretinide: a prototype cancer prevention drug. *Expert Opin Invest Drugs* 12:1829–42

Maurer BJ, Melton L, Billups C *et al.* (2000) Synergistic cytotoxicity in solid tumor cell lines between N-(4-hydroxyphenyl)retinamide and modulators of ceramide metabolism. *J Natl Cancer Inst* 92:1897–909

Miller LA, Goldstein NB, Johannes WU *et al.* (2009) BH3 mimetic ABT-737 and a proteasome inhibitor synergistically kill melanomas through Noxa-dependent apoptosis. *J Invest Dermatol* 129:964–71

Mohana-Kumaran N, Hill DS, Allen JD *et al.* (2014) Targeting the intrinsic apoptosis pathway as a strategy for melanoma therapy. *Pigment Cell Melanoma Res* 27:525–39

Monzani E, Facchetti F, Galmozzi E *et al.* (2007) Melanoma contains CD133 and ABCG2 positive cells with enhanced tumourigenic potential. *Eur J Cancer* 43:935–46

Oltersdorf T, Elmore SW, Shoemaker AR *et al.* (2005) An inhibitor of Bcl-2 family proteins induces regression of solid tumours. *Nature* 435:677–81

Placzek WJ, Wei J, Kitada S *et al.* (2010) A survey of the anti-apoptotic Bcl-2 subfamily expression in cancer types provides a platform to predict the efficacy of Bcl-2 antagonists in cancer therapy. *Cell Death Dis* 1:e40

Ramirez-Labrada A, Lopez-Royuela N, Jarauta V *et al.* (2014) Two death pathways induced by sorafenib in myeloma cells: Puma-mediated apoptosis and necroptosis. *Clin Transl Oncol*; e-pub ahead of print 19 July 2014

Reginato MJ, Mills KR, Paulus JK *et al.* (2003) Integrins and EGFR coordinately regulate the pro-apoptotic protein Bim to prevent anoikis. *Nat Cell Biol* 5:733–40

Reuland SN, Goldstein NB, Partyka KA *et al.* (2011) The combination of BH3-mimetic ABT-737 with the alkylating agent temozolomide induces strong synergistic killing of melanoma cells independent of p53. *PLoS One* 6:e24294

Reuland SN, Goldstein NB, Partyka KA *et al.* (2012) ABT-737 synergizes with Bortezomib to kill melanoma cells. *Biol Open* 1:92–100

Ribble D, Goldstein NB, Norris DA *et al.* (2005) A simple technique for quantifying apoptosis in 96-well plates. *BMC Biotechnol* 5:12

Roesch A, Fukunaga-Kalabis M, Schmidt EC *et al.* (2010) A temporarily distinct subpopulation of slow-cycling melanoma cells is required for continuous tumor growth. *Cell* 141:583–94

Roesch A, Vultur A, Bogeski I *et al.* (2013) Overcoming intrinsic multidrug resistance in melanoma by blocking the mitochondrial respiratory chain of slow-cycling JARID1B(high) cells. *Cancer Cell* 23:811–25

Santini R, Vinci MC, Pandolfi S *et al.* (2012) Hedgehog-GLI signaling drives self-renewal and tumorigenicity of human melanoma-initiating cells. *Stem Cells* 30:1808–18

Shakhova O, Sommer L (2013) Testing the cancer stem cell hypothesis in melanoma: the clinics will tell. *Cancer Lett* 338:74–81

Smith SM, Ribble D, Goldstein NB *et al.* (2012) A simple technique for quantifying apoptosis in 96-well plates. In: PMC (eds) *Laboratory Methods in Cell Biology*. 1st edn. Elsevier Inc.: Chennai, India, 361–8

Soengas MS, Lowe SW (2003) Apoptosis and melanoma chemoresistance. *Oncogene* 22:3138–51

Stecca B, Santini R, Pandolfi S *et al.* (2013) Culture and isolation of melanoma-initiating cells. *Curr Protoc Stem Cell Biol* Chapter 3:Unit 3 6

Tentler JJ, Tan AC, Weekes CD *et al.* (2012) Patient-derived tumour xenografts as models for oncology drug development. *Nat Rev Clin Oncol* 9:338–50

Thomas S, Quinn BA, Das SK *et al.* (2013) Targeting the Bcl-2 family for cancer therapy. *Expert Opin Ther Targets* 17:61–75

Torrisi R, Decensi A (2000) Fenretinide and cancer prevention. *Curr Oncol Rep* 2:263–70

Wong CY, Helm MA, Kalb RE *et al.* (2013) The presentation, pathology, and current management strategies of cutaneous metastasis. *N Am J Med Sci* 5:499–504

Zhang H, Mi JQ, Fang H *et al.* (2013) Preferential eradication of acute myelogenous leukemia stem cells by fenretinide. *Proc Natl Acad Sci USA* 110:5606–11